# Elimination of interferences in enzyme-based potentiometric sensors

Ivan Magriñá Lobato

Nanoscience, Materials and Processes: Chemical Technology at the Frontier Master Program 2014-2015

ivan.magrina@estudiants.urv.cat


Supervisor: Francisco J. Andrade

Department of Analytical Chemistry and Organic Chemistry. Universitat Rovira i Virgili

Campus Sescelades, c/ Marcel·lí Domingo, 1. Tarragona, 43007, Spain.

## Abstract

An approach for the elimination of interferences in an enzyme-based potentiometric glucose biosensor based on the oxidation of the interferences by using nanostructured $MnO_2$ is presented. Two different strategies were evaluated: i) direct addition of $MnO_2$ to the sample followed by filtration and, ii) immobilization of $MnO_2$ over the glucose biosensor as a pre-oxidizing layer. Both strategies have been successfully tested in real samples and these preliminary results have been validated against a commercial glucometer. Additionally, these results suggest that method for the elimination of interferences presented here could be potentially applied to other enzyme-based potentiometric sensors.


Keywords: potentiometry, biosensor, interference elimination, glucose, $MnO_2$ nanoparticles.
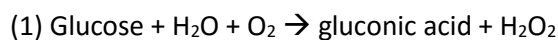
## Introduction

Clinical diagnostics and frequent health monitoring are essential for the early detection of diseases and further control and management of clinical conditions. However, most of these activities have been traditionally centralized in lab facilities because the analytical techniques employed are bulky, expensive, and need properly trained personal. The usual process for a clinical analysis starts when the patient visits the doctor for the prescription. Thereafter, patients must book a sample extraction date, then the sample is sent to the lab, the analysis is performed, the result come back to the doctor and then the patient is called to receive the results. Consequently, the clinical information is usually obtained days after sample extraction, limiting the decision-making capacity of doctors. All in all, the process is tedious for the patient and consumes significant amount of resources from the healthcare system. Furthermore, in the case of conditions such as diabetes, delays in the information may be life-threatening. To overcome this problem, miniaturized, accurate and affordable analytical devices have been developed during the last decades. Those devices, often called point-of-care devices, allow to obtain accurate and relevant clinical information in a short period of time, improving the clinical diagnosis and also the health monitoring in chronic diseases.[1]

Back in 1971, Clemens developed and patented one of the first examples of a successful self-monitoring point-of-care device, a colorimetric glucometer.[2] With the time, glucometers have moved to amperometric detection, because it provides more advantages than colorimetry, such as, high sensitivity, a wider linear range, a reasonable low price, simplicity and the possibility of miniaturization.[3] Apart from glucose, other clinical biosensors have been developed to detect other analytes, such as, lactate[4], choline[5], ethanol[6], or glutamate[7], to mention just a few. Nowadays, while amperometric enzyme based biosensors are the most prevalent point-of-care devices in the market, there is a significant research activity in order to find suitable alternatives.

Potentiometric sensors are gaining increasing interest as an attractive alternative to develop new enzymatic point-of-care devices, especially in the developing countries, where the economic constrains and infrastructure limitations are higher. Potentiometry is one of the oldest electrochemical techniques, and it is still in use in clinical diagnostics for many reasons. The instrumentation is simple, robust, compact and affordable and has low power consumption. The working principles of the potentiometric measurements are well established[8]. In short, the difference of potential between a reference electrode and a working electrode is measured at almost zero current condition, i.e., open circuit potential. This difference of potential can be correlated with the analyte concentration in the sample. Usually, charged molecules are required to produce a change in potential in the working electrode. For that reason, potentiometry has been traditionally associated to the determination of charged ions, such as, $H^+$, $Li^+$, $Na^+$, $K^+$, $Cl^-$, $NH_4^+$, $Ca^{+2}$, $Mg^{+2}$ [9,10] etc., in bodily fluids. However, potentiometry can also be used to determine clinical relevant neutral molecules. One of the most known approaches is the use of an enzyme, which is used in order to produce a charged molecule from its substrate that then is recognized by the working electrode. For example, urea[11] and creatinine[12] can been determined using a pH working electrode coated with an urease or a creatininase/creatinase membrane, respectively, because both enzyme systems generate $NH_3$ as a product, changing the local pH of the working electrode surface.[13]

Additionally, neutral molecules can also be determined potentiometrically if a redox-active molecule is generated by an enzyme when a redox sensitive material –such as gold, palladium or platinum- is employed as working electrode.[14,15] This concept has been reported and patented back in 1988 by Schiller *et al.*[16] In their work, they developed a $H_2O_2$ sensitive electrode by coating a platinum working electrode with an acrylamide membrane and glucose oxidase, which produces $H_2O_2$ from glucose according to the reaction (1):

$$(1)\ Glucose + H_2O + O_2 \rightarrow gluconic\ acid + H_2O_2$$

This type of enzyme potentiometric sensor based on platinum transducer could be extended to other relevant analytes such as oxalate, D-glutamate, galactose or cholesterol, to mention just a few, due to the availability of their respective oxidases.

It is evident that, considering the massive revolution in nanotechnology, electronics and electrochemistry of the last 3 decades, the approach presented by Schiller *et al.* [16] can be revisited and redesigned in order to create a low-cost potentiometric sensor to determine clinically relevant neutral molecules in real samples. This path has been followed by Willander et al., who during the last few years have explored the development of nanostructured materials associated to enzymes for the potentiometric detection of biomolecules –glucose among them-[17,18]. While this approach has some limitations regarding the cost and size of the electrodes, the most severe problem, i.e., the sensitivity towards interferences that are normally present in real samples, has not been yet addressed. In a previous work, our group has presented as a model a glucose sensor, where the limitations of cost and size have been also overcome. The cost of the electrode was significantly reduced by using paper as a substrate instead of the more expensive traditional approaches that use glassy carbon or silicon-based materials. Paper is an attractive option because of its inherent low cost and optimal mechanical properties.[19] The amount of platinum required to build the electrode was also significantly reduced by sputtering a thin layer (50 nm) of this material over the paper. However, the cost of the sputtering is still relatively high and it could be reduced if a carbon nanotube ink –or any other cheaper conductive material- could be sensitized with platinum nanoparticles[20]. In addition, the use of a carbon nanotube ink could open the door for a mass production via direct or screen printing, reducing the electrode fabrication cost even further. Regarding the electrode miniaturization, the paper glucose sensor was designed following the typical approach used for construction of electrodes of the paper-

based ISEs previously developed in our group.[21] Finally, the problem regarding interferences present in real samples remained unsolved in that master thesis and this is the starting point of this work.

Previous works to remove interferences in amperometric enzyme sensors have been reported but, to the best of our knowledge, there are no studies regarding the elimination of interferences in potentiometric enzyme sensors using platinum as transducer. To face this problem, two strategies already applied to remove interferences in amperometric enzyme sensors could be potentially applied in potentiometric enzyme sensors: the use of permselective membranes or the oxidation of the interference.[22] Permselective membranes prevent interferences to reach the electrode surface by size exclusion and/or by electrostatic repulsion. Electropolymerized films made of poly/phenylendiamine, polyphenol and poly(aminophenol)[23,24] are able to satisfactory remove interferences by size exclusion while Nafion® is the polymer widely used to avoid interferences by electrostatic repulsion.[25] However, in both cases, the response time of the electrode is usually increased and the interferences are not completely avoided.[22] The other strategy that can be applied is the interference elimination by oxidation. Cha $et$ $al.$[26] incorporated insoluble oxides: $BaO_2$, $CeO_2$, $MnO_2$ and $PbO_2$ into cellulose acetate membrane to create a pre-oxidizing layer over a glucose amperometric sensor, proving that $MnO_2$ and $PbO_2$ were able to reduce redox active interferences. However, it was found that $MnO_2$ migrated from the membrane to the electrode decreasing the sensor sensitivity. Further studies performed by Chen $et$ $al.$[27] demonstrated that $MnO_2$ nanoparticles can be immobilized into a chitosan membrane to remove the interferences in a glucose amperometric sensor and avoid the migration problem found by Cha $et$ $al.$[26] As it was mentioned above, all these sensors used an amperometric detection approach.

In this work two approaches for the elimination of redox-active interferences present in real samples by using $MnO_2$ nanoparticles as chemical oxidant in an enzyme-based potentiometric glucose sensor are described. Results show that both approaches can effectively remove the adverse effect of the interferences and are viable and potentially transferable to other enzyme-based potentiometric sensors.

## Experimental

### Reagents and materials

Medium molecular weight chitosan (78-85% deacetylated), poly(vinyl alcohol) ($M_w$=89.000-98.000), glucose oxidase from $A.$ $niger$ (100.000-250.000 U/g), analytical grade salts NaCl, $NaHCO_3$, $K_2HPO_4$, $MgCl_2 \cdot 6H_2O$, $Mn(CH_3COO)_2 \cdot 4H_2O$ and $KMnO_4$, BioXtra grade D-(+)-Glucose, reagent grade sodium ascorbate, USP grade 4-acetaminophen, uric acid and bilirubin were obtained from Sigma-Aldrich. Phosphate buffered saline (PBS) 100 mM was prepared with 137 mM NaCl, 101,4 mM $Na_2HPO_4$, 17,6 mM $KH_2PO_4$, and 26,8 mM KCl. pH was adjusted with 1 M NaOH or 1 M HCl solutions.

Artificial serum was prepared with 111 mM NaCl, 29 mM $NaHCO_3$, 2,2 mM $K_2HPO_4$ and 0,8 mM $MgCl_2 \cdot 6H_2O$. pH was adjusted with 1 M NaOH or 1 M HCl solutions.

Glass microfiber filter 934-AH Whatman™ (1,5 μm pore size) and number 5 qualitative filter paper Whatman™ (2,5 μm pore size) were purchased from Sigma-Aldrich. Polyester mask with acrylic adhesive (ARcare 8259, adhesive research) was obtained from In. Limerick (source, Ireland).

All solutions were prepared with double distilled water (18,2 MΩcm$^{-1}$ specific resistance).

### Instrumentation and measurements

The sputtering of Platinum over filter paper was performed with a RF magnetron ATC Orion 8-HV from AJA International Inc. (MA, USA) operated at 150W and 3 mTorr of pressure in Argon.

Glucose membrane deposition was performed using a CHI660C Electrochemical Workstation from CH Instruments, Inc. (Austin, U.S.A) furnished with a glassy carbon counter electrode (CE), a single junction 3M Ag/AgCl/KCl from Metroohm AG

(Herisau, Switzerland) a reference electrode (RE) and the paper electrode used as a working electrode (WE).

Potentiometric measurements were carried out at room temperature (around 30ºC) with a high input impedance EMF16 multichannel potentiometer data acquisition device from Lawson Laboratories, Inc. (Malvern, USA). A double-junction 3M Ag/AgCl/KCl from Metrohm® AG (Herisau, Switzerland) containing 1M LiAc as a bridging solution was used as reference electrode (RE).

Environmental scanning electron microscopy (ESEM) images were obtained with a Quanta 200 (FEI, Oregon, USA) and the transmission electron microscopy (TEM) images were obtained using a JEOL model 1011 (JEOL USA Inc.).

Centrifugation was carried out using an EBA20 centrifuge from, Hettich Zentifugen, Germany.
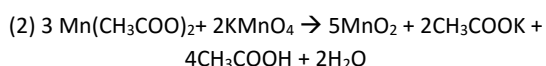
Ultrasonication was performed in a FB11205 ultrasonicator bath from Fisherbrand, Germany.

**MnO$_2$ synthesis**

Two different MnO$_2$ suspensions were prepared with different final particles sizes. To differentiate them they will be named MnO$_2$ "coarse" and MnO$_2$ "fine".

MnO$_2$ coarse

To prepare a MnO$_2$ coarse nanoparticle suspension, the protocol described by Xu et al.[27] was followed with some modifications. In summary, 40 ml KMnO$_4$ 100 mM were added to 4 ml Mn(CH$_3$COO)$_2$ 1,5 M and sonicated at 37 KHz during 1 hour at room temperature to allow the reaction to take place:

$$(2)\ 3\ Mn(CH_3COO)_2 + 2KMnO_4 \rightarrow 5MnO_2 + 2CH_3COOK + 4CH_3COOH + 2H_2O$$

Then, the suspension was centrifuged at 6.000 rpm during 15 minutes. The supernatant was discarded and the pellets were re-suspended with 40 ml of deionized water and centrifuged again. This process was repeated until neutral pH of the supernatant was obtained.  Finally, the pellet was re-suspended in deionized water to a final concentration of 20 mg/ml and the suspension was ultrasonicated during 15 minutes at 37 KHz. The suspension was stored at 4ºC.

Figure 1 shows a TEM image of MnO$_2$ coarse nanoparticle suspension obtained where it can be observed that, while the presence of nanoparticles is evident, they tend to form micron-sized aggregates.
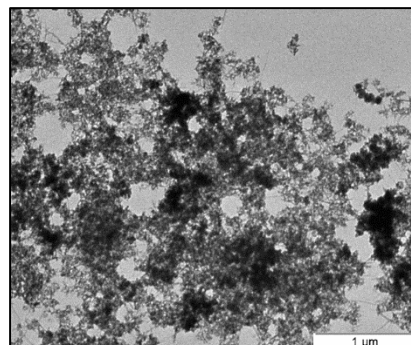


**Figure 1.** TEM image of MnO$_2$ coarse nanoparticles suspension.

MnO$_2$ fine

To prepare a MnO$_2$ fine nanoparticles suspension, the protocol described by Dontosova E. et al. (2011)[28] with some modifications was followed. In summary, 250 ml KMnO$_4$ 25 mM were added to 250 ml Mn(Ac)$_2$ 37,5 mM and stirred at room temperature during 5 minutes to allow the reaction (2) to take place. Then, the suspension was vacuum filtered using a Whatman$^{TM}$ 934-AH glass microfiber filter.  The cake was washed twice with 50 ml of deionized water and dried overnight at room temperature. Finally, the dried cake was re-suspended in deionized water to a final concentration of 20 mg/ml. The suspension was stored at 4 ºC before use. From  the TEM images shown in Figure 2, the MnO$_2$ nanoparticles produced present  wrinkle lamellar structures with estimated thickness of 0,3-0,6 nm and characteristic dimension 50-120 nm.[28]  However, the nanoparticles tend to aggregate in clusters that reach up to some microns in size.
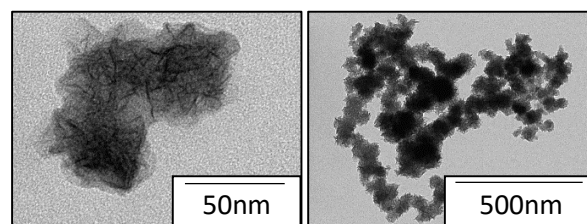


**Figure 2.** TEM images of MnO$_2$ fine nanoparticles suspension.

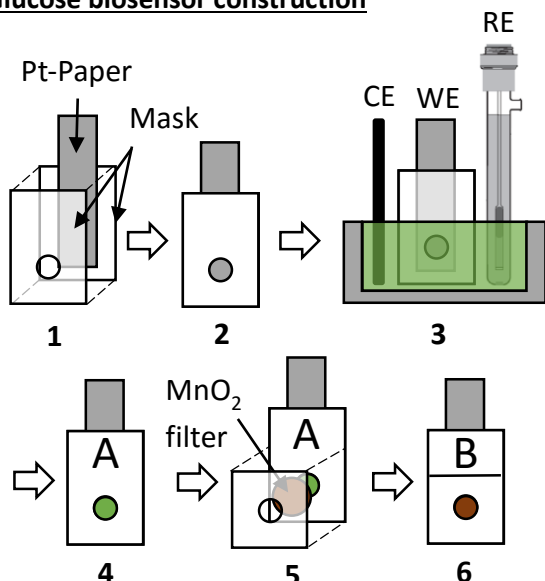## Glucose biosensor construction



**Figure 3.** A scheme of glucose sensor A and glucose sensor B construction. The image illustrates that Sensor B is a further modification of Sensor A.

Sensor A: Glucose sensor

A chitosan solution was prepared by stirring 1 g of chitosan in 100 ml of deionized water and 1 ml of glacial acetic acid at 90 ºC until the solution was clear. Poly(vinyl alcohol) (PVA) solution was prepared by dissolution of 1 mg of PVA in deionized water at 90 ºC until the solution was clear.

The glucose sensor was constructed on platinized filter papers. A Whatman™ number 5 qualitative filter paper was sputtered on one side with platinum in order to deposit a layer of approximately 50 nm. Then, the platinized paper was cut in 2 cm x 0,5 cm strips and they were sandwiched and glued between two 1,5 cm x 1 cm polyester mask strips. One of the mask strips contained a circular window of 3 mm diameter to expose the platinized paper (steps **1** and **2,** Figure 3). After this, the electrodes were immersed into a cocktail containing 3,5 mg of glucose oxidase, 1 ml Poly(vinyl alcohol) (1% wt.) and 2,5 ml of chitosan (1% wt.) and a membrane was electropolymerized onto the platinized surface by applying a current of 25 µA during 300 s (step **3,** figure 3). The resulting glucose sensor A was washed with artificial serum at pH 7,4, and finally dried and stored at 4 ºC during 24 h before use (step **4,** Figure 3).

Sensor B: Glucose sensor + $MnO_2$ membrane

A Whatman™ number 5 qualitative filter paper was used to vacuum filter 10 ml of a $MnO_2$ suspension (1 mg/ml). Then, the cake was washed twice with 25 ml of deionized water and the filter paper was dried at room temperature overnight and cut into 4 mm diameter circles. The paper circles were placed on glucose sensor A and glued with 1 cm x 1 cm mask containing a 3 mm window (see steps **5** and **6**, Figure 3).

Figure 4 shows that $MnO_2$ nanoparticle aggregates are heterogeneously distributed in only one side of the filter paper. This paper side should face the sample to preoxidize interferents and the side without nanoparticles should face the enzymatic layer to avoid $H_2O_2$ decomposition.
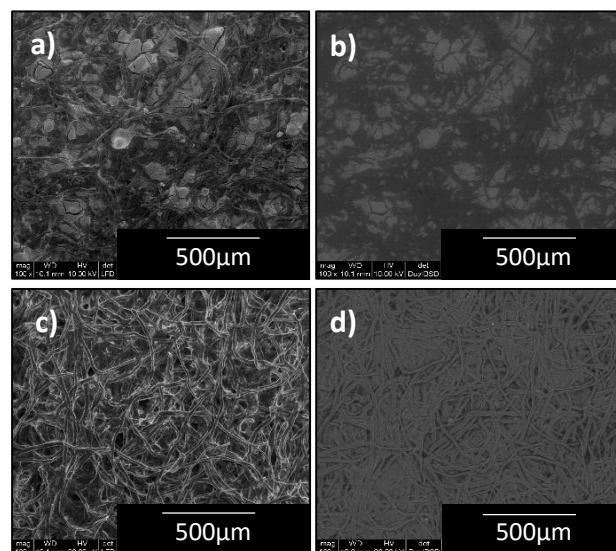


**Figure 4.** ESEM images of filter paper used to filter $MnO_2$ fine nanoparticle suspension. a) and c) are secondary electron images from both sides of filter paper while b) and d) are the corresponding backscattered electrons image.

## Results and discussion

### Sensor A: Glucose sensor

The composition of the glucose sensing membrane was optimized by changing the amount of enzyme in the electropolymerization cocktail and the parameters –potential, current and time- applied for the electropolymerization. The optimum conditions found - those that provide a higher sensitivity and a linear range closer to the clinical range of glucose in

blood/serum are those already mentioned in the experimental part.

## Sensor A: analytical performance

Sensor A performance was studied in artificial serum at 30±1 ºC. The sensor shows a sensitivity of -57±4 mV per decade, a limit of detection (LOD) of $10^{-4,2}$ M of glucose and a linear range from $10^{-3,5}$ M to $10^{-2,5}$M, as shown in Table 1. Details of the time-trace potentiometric response of sensor A and the corresponding calibration plot are shown in Figure 5. Glucose levels in blood/serum range from $10^{-2,4}$ M to $10^{-1,7}$ M, therefore, a sample dilution would be required if glucose levels need to be directly monitored in blood or serum samples using sensor A.
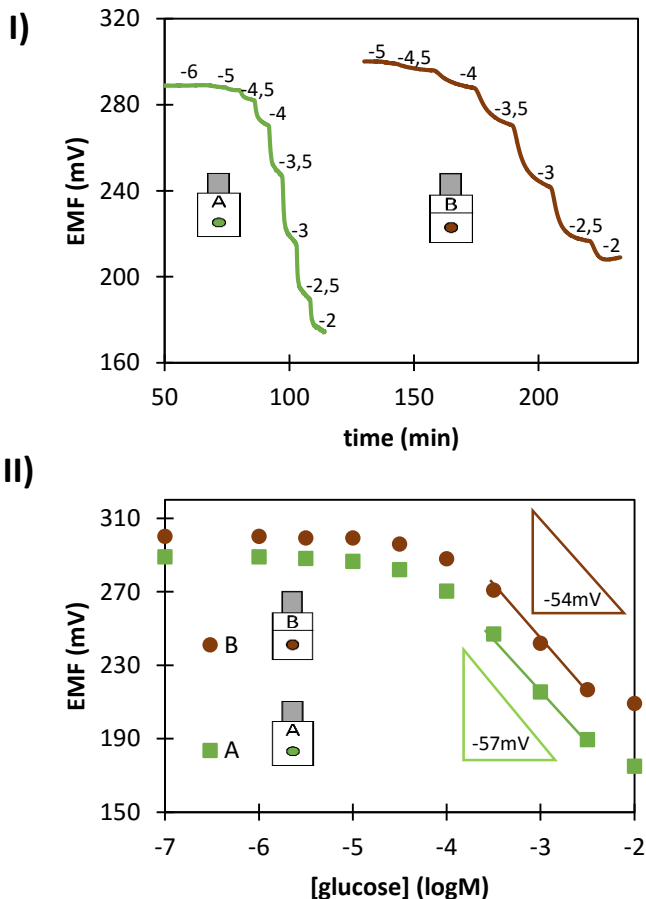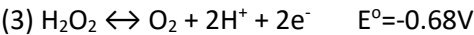


**Figure 5.** Potentiometric response for sensor A and B. I) the time-trace, and II) corresponding calibration plot, upon increasing glucose concentration are shown. The inset numbers in I) correspond to the logarithm of the concentration of glucose added

**Table 1.** Sensor analytical performance for the determination of glucose in PBS

|  | Sensor A | Sensor B |
|---|---|---|
| **Sensitivity (mV/dec)** | -57±4 | -54±5 |
| **LOD (M)** | $10^{-4,2}$ | $10^{-4}$ |
| **Linear range (M)** | $10^{-3,5}$ - $10^{-2,5}$ | |
| **Time of response (min)** | ≈5 | <15 |

Wingard et al.[14] suggest that the source of the potentiometric response is related to redox reactions on the platinum electrode surface occurring due to the presence of hydrogen peroxide produced by the enzyme. According to the Nernst equation[8], and taking into account the 2 electrodes involved in the hydrogen peroxide reduction (3), a slope of -29.6 mv/decade is expected.

$$(3)\ H_2O_2 \leftrightarrow O_2 + 2H^+ + 2e^- \qquad E^o = -0.68V$$

However, the slope obtained is significantly higher than expected (approximately -57 mV/decade, as shown in Table 1) and this difference can be explained by several factors that affect the response of the Pt electrode. Indeed, it is well known that there is complex set of reactions between $H_2O_2$ and Pt whose full nature is still not well understood. From the adsorption of oxygen on the Pt surface to the formation of complexes, there is a whole of set of complex physical and chemical process that are still under research. Furthermore, it has been reported that the potentiometric response is also dependent on the pretreatment in the platinum surface. [14] In our case, the platinum was sputtered on the filter paper and no pretreatment -apart from membrane deposition- was performed.

## Sensor A: interferents

The influence of four common redox interferences present in blood/serum samples was evaluated and results are shown in Figure 6. Among the interferences, bilirubin and acetaminophen slightly

affect the baseline potential. However, ascorbate and uric acid show the most severe interference.

It is well known that ascorbate and uric acid, the most important antioxidants presents in blood, are redox active species that are oxidized on the platinum electrode triggering a change in potential that could mask the glucose signal. Ascorbate is a particular interference, because it triggers the biggest change in potential, at the lowest concentration.
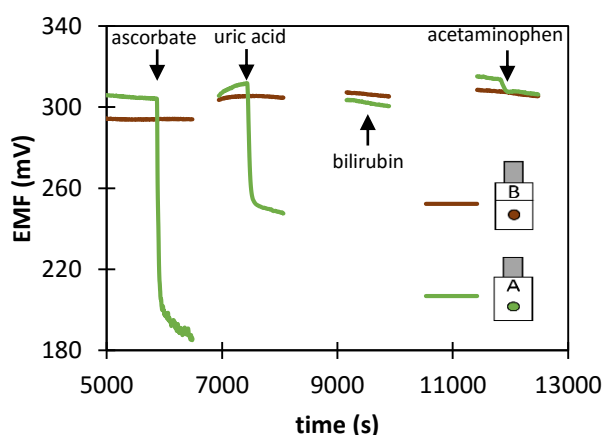


**Figure 6.** Time-trace of the potentiometric response for electrodes A and B to the presence of common redox interferences present in blood at blood levels: ascorbate 100 µM, uric acid 0,5 mM, bilirubin 1,5 mM, acetaminophen 120 µM.
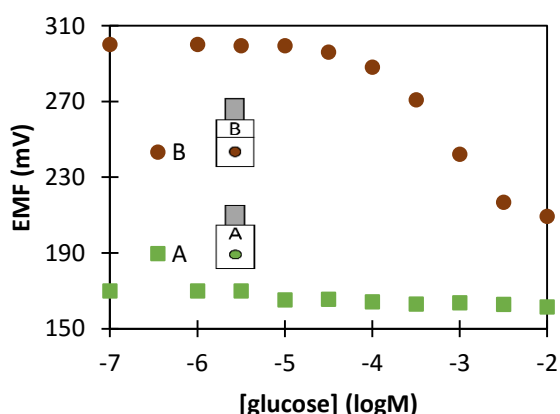


**Figure 7.** Glucose calibration plot with sensors A and B in artificial serum in presence of ascorbate 100µM.

In order to evaluate the ability of sensor A to determine glucose in the presence of interferences, a calibration curve for glucose was performed in artificial serum containing ascorbate 100 µM. As

shown in Figure 7, sensor A only responds to the presence of ascorbate and no change in potential is produced due to the increased concentration of glucose. This makes sensor A inviable to directly measure glucose in real samples unless interferences are removed or avoided.

Sensor A: Interference preoxidation with $MnO_2$

In order to make sensor A viable to measure glucose in real samples, $MnO_2$ was used as chemical oxidant to remove interferences.

To demonstrate that glucose levels can be determined in presence of interferences when $MnO_2$ is used to pre-oxidize the sample, three different samples were prepared in PBS 100 mM at pH 7,4: a) glucose 5 mM, b) ascorbate 100 µM and c) glucose 5mM + ascorbate 100 µM. Samples were prepared by duplicate. One replica was pre-oxidized with 0,1 mg/ml $MnO_2$ coarse nanoparticle suspension and filtered with syringe acetate filter 0,45 µm pore size before potentiometric measurements. The other replica, called blank, was directly measured in the potentiometer. The potentiometric response time-trace is shown in Figure 8. From sample a) can be concluded that $MnO_2$ preoxidation does not affect glucose because the potential value obtained in both cases, pre-oxidized sample and blank, is the same. From sample b) can be concluded that $MnO_2$ can successfully oxidize ascorbate because potential value obtained from pre-oxidized ascorbate sample is similar to the potential value of PBS solution. In contrast, the not pre-oxidized ascorbate sample presents a change in potential around 120 mV, which can be attributed to the presence of ascorbate. Finally, from sample c) can be concluded that samples containing interferences can be successfully oxidized to measure glucose levels because the potential value obtained is equal to the glucose levels in a). In contrast, if sample containing glucose and ascorbate is not preoxidized (c, blank) the potential value obtained corresponds to the potential of ascorbate.

To conclude, $MnO_2$ was successfully used to pre-oxidize samples and remove interferences. It can also

be also observed that the products generated by the oxidation of the interferences do not trigger a change in the sensor potentiometric response.
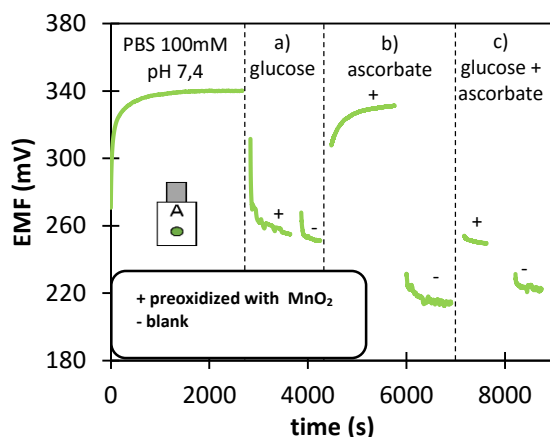


**Figure 8.** Time-trace potentiometric response of sensor A to different samples: a) glucose 5mM, b) ascorbate 100 μM, and c) glucose 5mM + ascorbate 100 μM.

Sensor A: Serum sample measurements

In order to test the ability of $MnO_2$ to remove interferences in real samples, sensor A was calibrated, and then serum samples preoxidized with 1 mg/ml $MnO_2$ fine/coarse nanoparticles and diluted 1:5 were placed on the potentiometric cell. The glucose concentrations were predicted using the calibration plot obtained. The same protocol was used to determine glucose concentration in 5 different serum samples (1 and 2 with $MnO_2$ large nanoparticles and 4, 5 and 6 with $MnO_2$ fine nanoparticles). To validate the results, an amperometric glucose sensor Countour XT from Bayer was used. In this case, serum samples were directly measured. Table 2 shows a result comparison using both methods.

**Table 2.** Concentration of glucose in serum samples predicted by sensor A and Contour XT glucometer.

| Sample | Sensor A mg/dL | Glucometer mg/dL | Error % |
|--------|--------|-----------|-------|
| 1 | 77 | 92 | -16 |
| 2 | 68 | 92 | -25 |
| 3 | 52 | 131 | -60 |
| 4 | 37 | 82 | -56 |
| 5 | 31 | 72 | -56 |

As shown in Table 3, the glucose concentration predicted by the sensor is lower than the glucose predicted by the glucometer, in all cases. This could be explained by a $MnO_2$ leakage through the filter, which is able to decompose the $H_2O_2$ peroxide produced by the enzyme, decreasing the corresponding glucose signal[27]. When larger nanoparticles are employed (1 and 2), the $MnO_2$ leakage and the error predictions are lower. Consequently, if this strategy is going to be used to remove interferences in real samples, $MnO_2$ nanoparticles should be avoided unless they form aggregates big enough to be retained by the filter. In any case, a small systematic error is always easier to correct, providing that the magnitude of the bias remains constant.

**Sensor B: Glucose sensor + $MnO_2$ membrane**
Another strategy used to eliminate interferences consists on the immobilization of $MnO_2$ on a porous membrane placed over the glucose sensor. Chitosan was successfully employed to immobilize $MnO_2$ by Chen *et al.* [27]. However, Cha et al. experimental conditions and alternative experimental conditions were tested unsuccessfully. Sensor sensitivity was usually decreased, reproducibility was poor and interferences were not completely removed. Other porous polymers compatible with enzymes, could be potentially used to immobilize nanoparticles, for example: agar or κ-carragenaan[29], however they were not studied in this work. Nevertheless, a simpler strategy leaded to an equal sensitivity, reproducibility and completely interference elimination at the cost of increased time of response. The strategy consisted on the immobilization of $MnO_2$ onto a filter paper by filtration, as shown in Figure 3.

Sensor B: analytical performance
As can be observed in Table 2, sensor B shows a sensitivity of -54±5 mV per decade, a LOD of $10^{-4}$ M and a linear range from $10^{-3,5}$ M - $10^{-2,5}$ M in artificial serum at 30 ºC which is comparable to sensor A performance. However, the time of response is

increased by a factor of 3, moving from 5 minutes to 15 minutes. Different filter papers with different pore sizes and thickness were tested to improve the time of response, however, no significant differences were found. Additionally, an electrode B without $MnO_2$ nanoparticles retained on the filter paper was employed to determine that increased time of response is not due to the immobilized $MnO_2$. This increment of the time of response is attributed to the fact that the extra filter paper membrane creates an extra layer where mass transfer equilibrium takes place.

Sensor B: interferences

The $MnO_2$ membrane present in sensor B completely remove interferences at usual blood levels as shown in Figure 6. In addition, glucose could be measured in presence of ascorbate using sensor B as shown in Figure 7. The results suggest that $MnO_2$ membrane solves the interference problem presented in sensor A while keeping the analytical performance. The only problem remaining, however, is the time of response.

Sensor B: measurements of serum sample

After calibration, serum samples diluted 1:5 were placed on the potentiometric cell and the glucose concentrations were predicted using the calibration plot obtained in sensor B. The glucose additions in the calibration curve were performed every 15 minutes while the sample was left in contact with the electrode during 1 hour. In between the calibration curve and the measurement of a serum sample, the electrode baseline potential needs to be recovered using artificial serum. The same protocol was used to determine glucose concentration in 5 different serum samples. To validate the results, an off-shelf commercial amperometric glucose sensor Countour XT from Bayer was used. In this case, the serum samples were directly measured. The comparison using both methods is shown in table 3.

**Table 3.** Concentration of glucose in serum samples predicted by sensor B and Contour XT glucometer.

| Sample | Sensor B mg/dL | Glucometer mg/dL | Error % |
|--------|--------|--------|--------|
| 1 | 97 | 88 | 10 |
| 2 | 108 | 88 | 22 |
| 3 | 66 | 74 | -10 |
| 4 | 72 | 74 | -3 |
| 5 | 69 | 81 | -14 |

As can be observed in Table 3, glucose levels can be predicted with an average error of +/- 15%. The error is acceptable according to ISO15197:2003 which allows a 20% error in 95% of all the samples.

However, from other experiments (results not shown here), it can be concluded that if $MnO_2$ large nanoparticles are used in the filter paper membrane, glucose values obtained were higher than expected because $MnO_2$ was heterogeneously distributed over the paper and the interferences were not completely removed. On the other hand, fine $MnO_2$ nanoparticles allowed a higher reproducibility between sensors and better interference elimination because the nanoparticles are better distributed over the filter paper membrane. However, when the $MnO_2$ filter paper remains more than 3 days in stock, nanoparticles get completely dry, and tend to form dust that can migrate through the paper filter to the electrode surface, reducing the sensor sensitivity. Therefore, the use of fresh $MnO_2$ filter papers to avoid $MnO_2$ leakage is recommended. Further work should be conducted in the future in order to immobilize the nanoparticles in a ways that their retention in the filter remains constant through longer periods of time.

## Conclusions

This work has successfully addresses the problem of the most sever interferences commonly found in potentiometric enzyme-based glucose sensor using platinum as a transducer.

The first step toward solving this problem using $MnO_2$ and both strategies using $MnO_2$ to avoid interferences are valid: a) pre-oxidize the sample

before measuring, b) integrate the $MnO_2$ into a membrane. However, further work is needed to fully optimize this approach.

Remarkably, this work suggests that both strategies could be applied to eliminate interferences in other enzyme based potentiometric sensors, giving an interesting perspective for a new bio-electrochemical sensing platform.

## REFERENCES

(1)  Chin, C. D.; Linder, V.; Sia, S. K. *Lab Chip* **2007**, *7* (1), 41.

(2)  Oliver, N. S.; Toumazou, C.; Cass, a. E. G.; Johnston, D. G. *Diabet. Med.* **2009**, *26*, 197.

(3)  Wang, J. *J. Pharm. Biomed. Anal.* **1999**, *19* (1-2), 47.

(4)  Bardeletti, G.; Sechaud, F.; R. Coulet, P. *Anal. Chim. Acta* **1986**, *187*, 47.

(5)  Xin, Q.; Wightman, R. M. *Anal. Chim. Acta* **1997**, *341* (1), 43.

(6)  Boujtita, M. *Biosens. Bioelectron.* **2000**, *15* (5-6), 257.

(7)  Wollenberger, U.; Scheller, F. W.; Böhmer, A.; Passarge, M.; Müller, H.-G. *Biosensors* **1989**, *4* (6), 381.

(8)  Bakker, E.; Bühlmann, P.; Pretsch, E. *Talanta* **2004**, *63* (1), 3.

(9)  Dimeski, G.; Badrick, T.; John, A. S. *Clin. Chim. Acta.* **2010**, *411* (5-6), 309.

(10) Oesch, U.; Ammann, D.; Simon, W. *Clin. Chem.* **1986**, *32* (8), 1448.

(11) Sehitogullari, A. *Talanta* **2002**, *57* (6), 1039.

(12) Pandey, P. C.; Mishra, A. P. *Sensors Actuators B Chem.* **2004**, *99* (2-3), 230.

(13) Koncki, R. *Anal. Chim. Acta* **2007**, *599*, 7.

(14) Lemuel B. Wingard Jr., J. C. *Biosensors Fundamentals and Applications*; Antony P. F Turner, Isao Karube, G. S. W., Ed.; 1987.

(15) Wingard, L. B.; Cantin, L. A.; Castner, J. F. *Biochim. Biophys. Acta* **1983**, *748* (1), 21.

(16) Liu, C.-C.; G. Schiller, J.; B. Wingard, L. United States Patent. 4340448, 1982.

(17) Usman Ali, S. M.; Nur, O.; Willander, M.; Danielsson, B. *Sensors Actuators, B Chem.* **2010**, *145* (2), 869.

(18) Khun, K.; Ibupoto, Z. H.; Lu, J.; AlSalhi, M. S.; Atif, M.; Ansari, A. A.; Willander, M. *Sensors Actuators B Chem.* **2012**, *173*, 698.

(19) Nery, E. W.; Kubota, L. T. *Anal. Bioanal. Chem.* **2013**, *405* (24), 7573.

(20) Zhao, Y.; Fan, L.; Zhong, H.; Li, Y. *Microchim. Acta* **2006**, *158* (3-4), 327.

(21) Novell, M.; Parrilla, M.; Crespo, G. a.; Rius, F. X.; Andrade, F. J. *Anal. Chem.* **2012**, *84* (11), 4695.

(22) Jia, W. Z.; Wang, K.; Xia, X. H. *TrAC - Trends Anal. Chem.* **2010**, *29* (4), 306.

(23) Palmisano, F.; Guerrieri, a; Quinto, M.; Zambonin, P. G. *Anal. Chim. Acta* **1995**, *67* (5), 1005.

(24) Chen, X.; Matsumoto, N.; Hu, Y.; Wilson, G. S. *Anal. Chem.* **2002**, *74* (2), 368.

(25) Anh, D. T. V.; Olthuis, W.; Bergveld, P. *Sensors Actuators B Chem.* **2003**, *91* (1-3), 1.

(26) Sung, H. C.; Sung, D. L.; Jae, H. S.; Ha, J.; Nam, H.; Geun, S. C. *Anal. Chim. Acta* **2002**, *461* (2), 251.

(27) Xu, J. J.; Luo, X. L.; Du, Y.; Chen, H. Y. *Electrochem. commun.* **2004**, *6* (11), 1169.

(28) Dontsova, E. a.; Zeifman, Y. S.; Budashov, I. a.; Eremenko, a. V.; Kalnov, S. L.; Kurochkin, I. N. *Sensors Actuators, B Chem.* **2011**, *159* (1), 261.

(29) Bezerra, C. S.; de Farias Lemos, C. M. G.; de Sousa, M.; Gonçalves, L. R. B. *J. Appl. Polym. Sci.* **2015**, *42125*, n/a.